Article ID: 1006-8775(2019) 04-0471-12

INTERANNUAL VARIABILITY OF WINTER–TO–SPRING CIRCULATION TRANSITION OVER SOUTHERN CHINA AND ITS SURROUNDING AREAS AND MECHANISMS

ZHOU Ming-sen (周明森), JIAN Mao-qiu (简茂球)
(1. Center for Monsoon and Environment Research/ Guangdong Province Key Laboratory for Climate Change and Natural Disaster Studies/ School of Atmospheric Sciences, Sun Yat-sen University, Guangzhou 510275 China;
2. Southern Marine Science and Engineering Guangdong Laboratory (Zhuhai), Zhuhai 519082, China)

Abstract: The climatological features and interannual variation of winter-to-spring transition over southern China and its surrounding areas, and its possible mechanisms are examined in this study. The climatological mean winter-to-spring transition is approximately in mid-March over southern China and the northern South China Sea. During the transition stage, anomalous southwest winds prevail at low-level over southern China and its nearby regions with enhanced convergence center over southern China, bringing more moisture from the Bay of Bengal(BOB) and the South China Sea(SCS) to southern China; meanwhile, the upper level is characterized by an obvious divergence wind pattern over southern China to the southwest part of Japan and enhanced upward motion. All the change of circulation is favorable to an increase of precipitation over southern China after seasonal transition. The winter-to-spring transition is predominantly on the interannual variation over southern China and the northern SCS. Early winter-to-spring transitions may induce more precipitation over southern China in spring, especially in March, while late cases will result in less precipitation. The interannual variability of the winter-to-spring transition and the related large-scale circulation are closely associated with the decaying phase of ENSO events. The warm ENSO events contribute to early winter-to-spring transitions and more precipitation over southern China.

Key words: winter-to-spring transition; southern China and its surrounding areas; interannual variability; mechanism; ENSO
CLC number: P461 **Document code:** A
doi: 10.16555/j.1006-8775.2019.04.005

1 INTRODUCTION

East Asia is under the influence of typical monsoon climate. It is cold and dry in winter with prevailing northerly winds of winter monsoon and is warm and humid in summer with prevailing southerly winds of summer monsoon (Chen and Jin [1]; Zhu et al. [2]; Tao and Chen[3]). The transition period from winter monsoon to summer monsoon is usually short. There are two kinds of opinions on the seasonal transition time from winter to summer in East Asia. One is that the winter-to-summer transition time of East Asian atmospheric circulation is in May, and just follows the onset of the South China Sea summer monsoon (SCSSM) (Lau and Yang [4]; Webster et al. [5]; Wang and Lin [6]; Wu et al. [7]). Although a persistent rain band appears in late March-early April in southern China, many researchers still classify it as spring precipitation (Tian and Yasunari [8]; Wan and Wu [9]; Zhao et al. [10]). The other opinion believes that the East Asian atmospheric circulation has changed from winter pattern to summer pattern before the SCSSM onset, suggesting the transition time in late March-early April (Jian et al. [11]; Qi et al. [12]; Zhu et al. [13]).

Many studies focus on the characteristics of the winter-to-summer atmospheric circulation transition in East Asia. Jian et al. [11] illustrated that the seasonal transition time of atmospheric heat sources from boreal winter to summer occurs in late March in the Asian-Australian Monsoon region. Qi et al. [12] found that the seasonal reversal of the zonal thermal difference between the East Asian continent and the western North Pacific occurs during late March to early April in the subtropical region, and the prevailing wind turns from northerly to southerly with the convective precipitation emerging simultaneously. Zhu et al. [13] revealed that the East Asian subtropical summer monsoon (EASSM) is established during the end of March to the beginning of April, using meridional wind to define the transition time of East Asian subtropical monsoon. In addition to above physical variables used to detect the seasonal transition time, the daily surface air temperature was also used to discriminate the seasonal cycles in China and spring onset

Received 2018-09-04; **Revised** 2019-08-06; **Accepted** 2019-11-15
Foundation item: National Key Basic Research Program of China (2014CB953901); Program of National Science Foundation of China (41475049); Fundamental Research Funds for the Central Universities (16lgjc05)
Biography: JIAN Mao-qiu, Professor, undertaking research on monsoon and regional climate.
Corresponding author: JIAN Mao-qiu, e-mail: eesjmq@mail.sysu.edu.cn

in northeast China (Yan et al. [14]; Zheng et al. [15]), and it was found that the local winter period has shortened and the local spring phase has advanced significantly in most of China. Furthermore, phenophases of woody plants also can be used for the detection of the timing of spring onset (Ho et al. [16]; Zheng et al. [17]). Springtime is a unique transition season from winter to summer in East Asian monsoon region, during which the seasonal climate changes rapidly. However, the characteristics and physical processes of winter-to-spring atmospheric circulation transition in East Asia, especially in southern China, are rarely involved in previous studies and remain to be investigated. The study of winter-to-spring atmospheric circulation transition will enhance the understanding of important processes that are responsible for the development of extreme climate events in spring in southern China.

Climatologically, the annual rainfall in southern China is above 1000 mm. In summer, the prevailing southwesterly wind brings sufficient warm moist air from low latitudes to southern China, causing abundant precipitation which accounts for 30–50% of the total annual rainfall. However, the spring rainfall over southern China can contribute 25–40% of the total annual precipitation, which is only second to the summer rainfall (Zhao et al.[10]; Wu and Qian[18]). Specifically, for southern China, it usually experiences a long rainy season from April to September, of which April-June is defined as annually first rainy season, and most widespread floods often occur in this period (Chen et al.[19]; Zhou [20]). Many studies have identified some major factors for the precipitation over southern China such as El Niño/Southern Oscillation (ENSO) (Zhang et al. [21]; Zhang et al. [22]; Wang et al. [23]; Wu et al. [24]; Wu et al. [25]; Zhou and Wu [26]), sea surface temperature (SST) anomalies in the South China Sea (SCS) and the Indian Ocean (Yang [27]; Zhou et al. [28]), snow cover in Tibetan Plateau (Wu and Qian[18]; Chen and Wu [29]), and the Arctic Oscillation (Gong et al. [30]). ENSO affects early-rainy season precipitation over southern China via a Rossby wave-type response of the Philippine Sea anticyclone caused by ENSO (Wang et al. [23]). Wu et al. [31] found that more summer rainfall over southern China corresponds to warm SST anomalies in the southeastern tropical Indian Ocean (SEIO) and cool SST anomalies in the central equatorial Pacific, which may force two anomalous vertical circulations with ascent bands over the SEIO and southern China and a common branch of descent over the SCS accompanied by an anomalous low-level anticyclone. The seasonal climate in southern China is closely dependent on the seasonal transition of circulation. Therefore, it is also worth exploring the connection between the precipitation of early-rainy season over southern China and the transition of spring-to-spring atmospheric circulation over southern China and its surrounding regions, to provide more precursory hints for the climatological prediction of precipitation over southern China.

The first aim of this study is to explore the transition characteristics of winter-to-spring circulation over southern China and its surrounding regions as well as their interannual variation. The relationship between seasonal transition and the precipitation over southern China, and its related processes are the second issue discussed in our study. Data and the analysis procedure are briefly introduced in section 2. Section 3 presents the spatiotemporal characteristics of winter-to-spring transition (WST) time. The influence of ENSO on WST is discussed in section 4. A summary is given in the last section.

2 DATA AND ANALYSIS METHODS

2.1 *Data*

The datasets used in the present study include: (1) monthly mean extended reconstructed SST (version v3b) provided by the National Oceanic and Atmospheric Administration (NOAA), available on 2 ° ×2° grid resolution (Smith et al. [32]); (2) ERA-Interim daily mean data from European Centre for Medium-Range Weather Forecasts (ECMWF), with a global coverage at a horizontal resolution of 1.5°×1.5° (Dee et al. [33]); (3) daily station observed precipitation data of 199 stations in southern China (south of 32° N and east of 110° E), provided by the National Meteorological Information Center (NMIC) of the China Meteorological Administration (CMA). The period of these datasets is adopted from 1979 to 2010.

2.2 *Methods*

Following Zeng and Zhang[34], a procedure measuring the similarity of two spatial patterns is adopted to identify the transition time of the atmospheric circulation from winter pattern to spring pattern. The procedure is introduced in detail as follows. Denoting the typical fields of variable F in winter and summer, represented by the climatological mean pattern in January and July, as $F_w=F(\theta, \lambda, P, t_1)$ and $F_s=F(\theta, \lambda, P, t_2)$, respectively. Letting

$$F^*=\frac{1}{2}(F_w+F_s), \tag{1}$$

and

$$\begin{cases} F'_w=F_w-F^* \\ F'_s=F_s-F^* \\ F'(\theta, \lambda, P, t)=F(\theta, \lambda, P, t)-F^* \end{cases} \tag{2}$$

The correlation coefficient $R_w(t)$ between F' and F'_w is expressed as

$$R_w(t)=(F'_w, F')/[\,\|F'\|\cdot\|F'_w\|\,]. \tag{3}$$

where the inner product $\|F'\|^2=(F', F')$, $(F'_w, F')=\frac{1}{s}\iint_s F'_w \cdot F' \mathrm{d}S$, $\|F'_w\|^2=(F'_w, F'_w)$, and S is the concerned domain

area. If the variable F' is a vector which can be written as $F'=u\vec{i}+v\vec{j}$, then the inner product turns to be a vector scalar product, i.e. $(F', F')=\frac{1}{s}\iint_s(u^2+v^2)\mathrm{d}S$. Then the four seasons are thus classified using the following criteria:

$$\begin{cases} 0.5<R_w(t)\leqslant 1, & \text{Winter} \\ -0.5<R_w(t)\leqslant 0.5, & \text{Spring or Autumn} \\ -1\leqslant R_w(t)<-0.5, & \text{Summer} \end{cases} \quad (4)$$

The procedure to identify the WST time (WSTT) is presented as follows: when R_w (t) falling from larger than 0.5 to smaller than 0.5, and in the following four pentads there is at least three pentads when R_w (t) is smaller than 0.5, then the first pentad with R_w (t) smaller than 0.5 is defined as the WST time, which also indicates the spring onset.

We also used Empirical Orthogonal Function (EOF) method, correlation analysis and composite analysis in this study. The statistical significance of these analyses is assessed using the two tailed Student's *t*-test. In this article, we define each five days from 1th January as a pentad, so each year has total 73 pentads (for leap year, 29 February is merged to the 12th pentad, which begins on 25 February and ends on 1 March).

3 SPATIOTEMPORAL CHARACTERISTIC OF WST

3.1 *Climatological distribution and interannual variation of WST*

Figure 1 shows the spatial pattern of climatological mean WSTT. For the Chinese mainland, the WSTT is fixed approximately at Pentad 15 over the southern coastal area of China and the northern SCS, mainly between 10° N and 25° N, while the distribution of the spring onset is rather complicated over central China. The WSTT is quite uniform over northern China, around Pentad 18. Like the coastal region of southern China, the transition time is also around Pentad 15 over a large area in the northwest Pacific. In the SCS, the WSTT is later over the southern SCS (3°–10°N) than over the northern SCS, because the difference between winter and spring is ambiguous over the tropical region, and there is not an obvious variation in tropics when the circulation in the northern SCS has a significant seasonal change. As shown in Fig. 2, the low-level wind direction over the southern SCS remains similar until Pentad 21, while the wind changes from northeasterly to easterly and the wind speed decreases over the northern SCS and coastal region of southern China during Pentads 12 to 15.

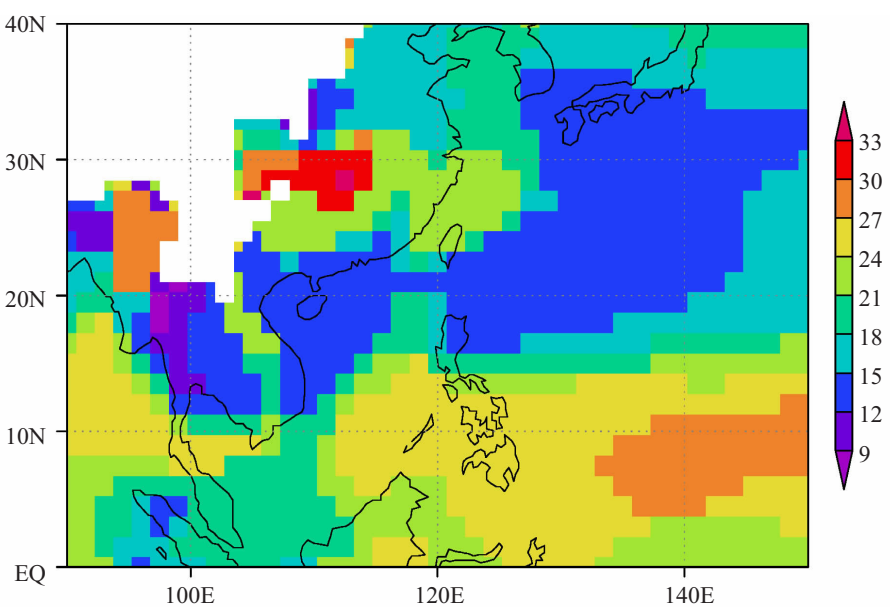

Figure 1. Climatological mean pattern of the winter-to-spring seasonal transition time (pentads) over East Asia during 1979–2010.

To capture the main characteristics of the WSTT interannual variability, the EOF analysis is applied to the WSTT in Asian monsoon region (60°E–150°E, 0°–50°N). The first three leading EOF modes account for 15.5%, 10.7% and 8.3% of the total variance, respectively. The first two modes are statistically distinguishable from the subsequent modes according to the rule given in North et al.[35]. The first EOF mode (EOF1) shows a seesaw pattern (Fig. 3a), with a positive center in the northern SCS and its surrounding regions and a negative extreme belt located in the south of the positive center, implying that the WSTTs over above two areas vary inversely with each other. EOF2 indicates a tripole pattern of 'negative-positive-negative' from southern China southeastward to its neighboring western tropical Pacific Ocean (Fig. 3c).

The first principal component (PC1) is predominant on the interannual time scale (Fig. 3b). According to a

criterion of 1.0 times of the standard deviation of PC1, we screen five early transition years (1983, 1987, 1992, 1998, and 2010) and six delayed transition years (1985, 1986, 1989, 1999, 2000, and 2009). All the five early transition years and five of the six delayed transition years (excluding 1986) are El Niño and La Niña decaying years, respectively. Thus, the interannual variation of the WSTT in the SCS and its surrounding regions is closely related to ENSO events. Similarly, PC2 is also predominant on the interannual time scale (Fig. 3d).

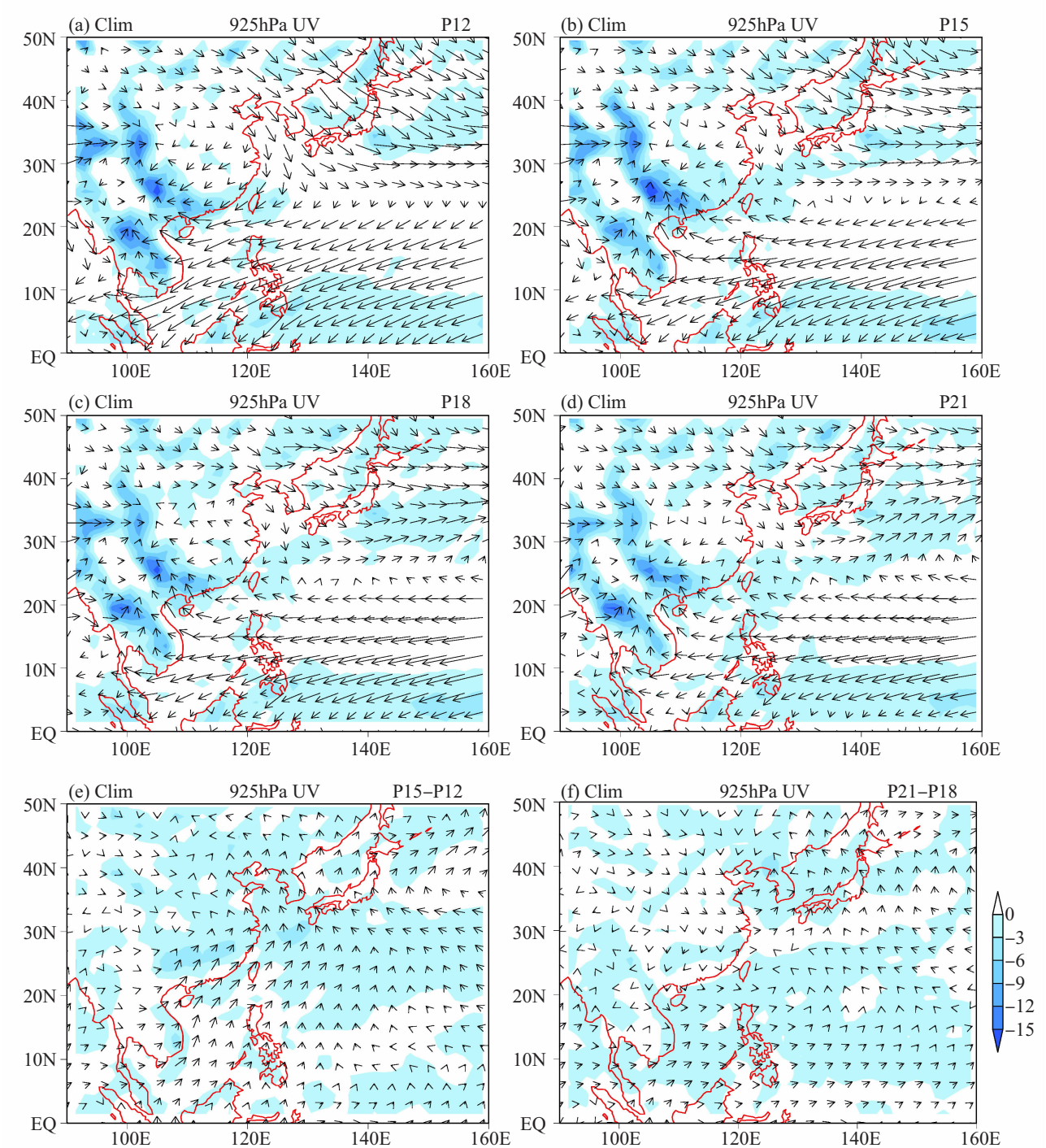

Figure 2. Climatological mean patterns of 925-hPa winds (vectors, m s^{-1}) and the divergence (shading, 10^{-6} s^{-1}) in 1979–2010. (a), (b), (c), and (d) are for Pentads 12, 15, 18, and 21, respectively. (e) Differences of wind and divergence between Pentad 15 and Pentad 12, and (f) differences between Pentad 21 and Pentad 18.

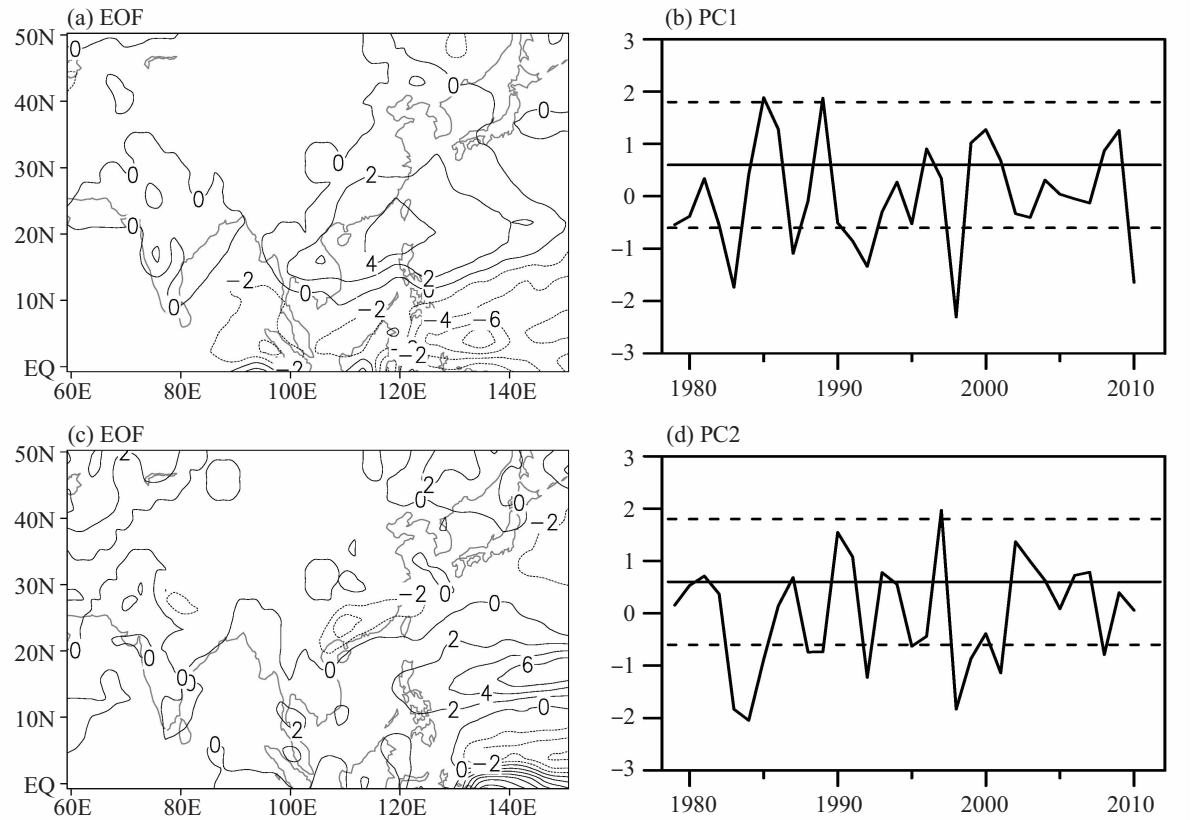

Figure 3. Spatial patterns of the (a) first and (c) second EOF modes of the normalized WSTT and their principal components (b) PC1 and (d) PC2 during 1979–2010.

3.2 *Characteristics of WST over the SCS and its surrounding regions and relationship between WST and precipitation*

3.2.1 CHANGES OF ATMOSPHERIC CIRCULATION DURING THE WST STAGE

Because the interannual variations of WSTT revealed by the first EOF mode are consistent in southern China and its adjacent ocean (SC-NSCS, 100°–140°E, 10°–30°N), for convenience, the area mean WSTT is estimated to discuss the seasonal transition characteristics. As shown in Fig. 4, the climatological WSTT is at Pentad 14 at 925 hPa, and at Pentad 26 at 200 hPa, respectively, with a correlation coefficient of –0.44 between them (significant at the 95% confidence level). Furthermore, the correlation coefficient between PC1 and the 925-hPa WSTT over the SC-NSCS is 0.6, implying the WSTT over the SC-NSCS appropriately representing the interannual variability of the first EOF mode. Therefore, based on the area-averaged WSTT at 925 hPa over the SC-NSCS, we will discuss the relationship between the WST and the circulation, and that between precipitation over southern China and seasonal transition.

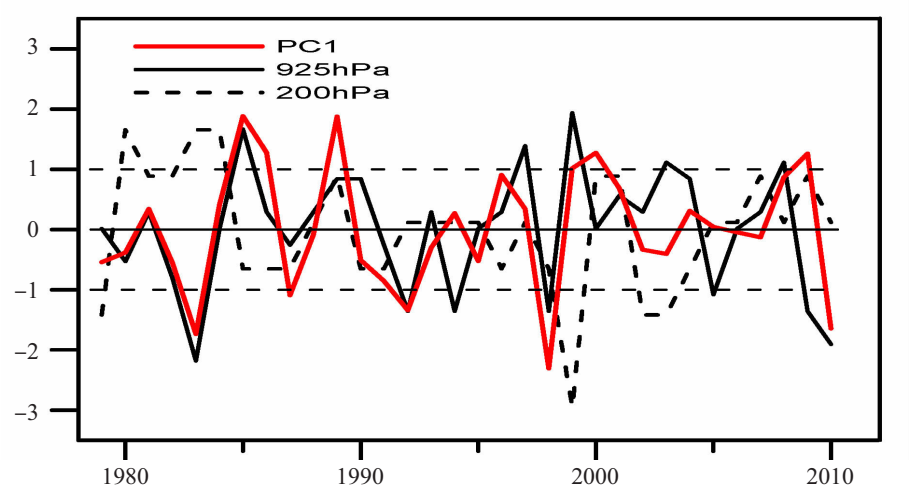

Figure 4. Normalized time series of area (100°–140°E, 10°–30°N) mean WST time anomalies at 925 hPa (solid black line) and 200 hPa (dashed line). Solid red line denotes PC1.

To better examine the features of atmospheric circulation change associated with the WST, we define the transition pentad as Pentad 0, and then perform composite differences of the winds averaged in two pentads before and after Pentad 0. The most significant change during the transition stage at low-level wind is the anomalous southwest winds over the SC and its nearby regions, with a distinct convergence center over southern China (Fig. 5a), which is conducive to the moisture transport from the BOB and SCS to southern China and the precipitation over there. Meanwhile, an obvious divergence wind pattern presents at 200-hPa, with a divergence zone over southern China to the southwest part of Japan (Fig. 5b) and enhancing upward motion over there (Fig. 5c).

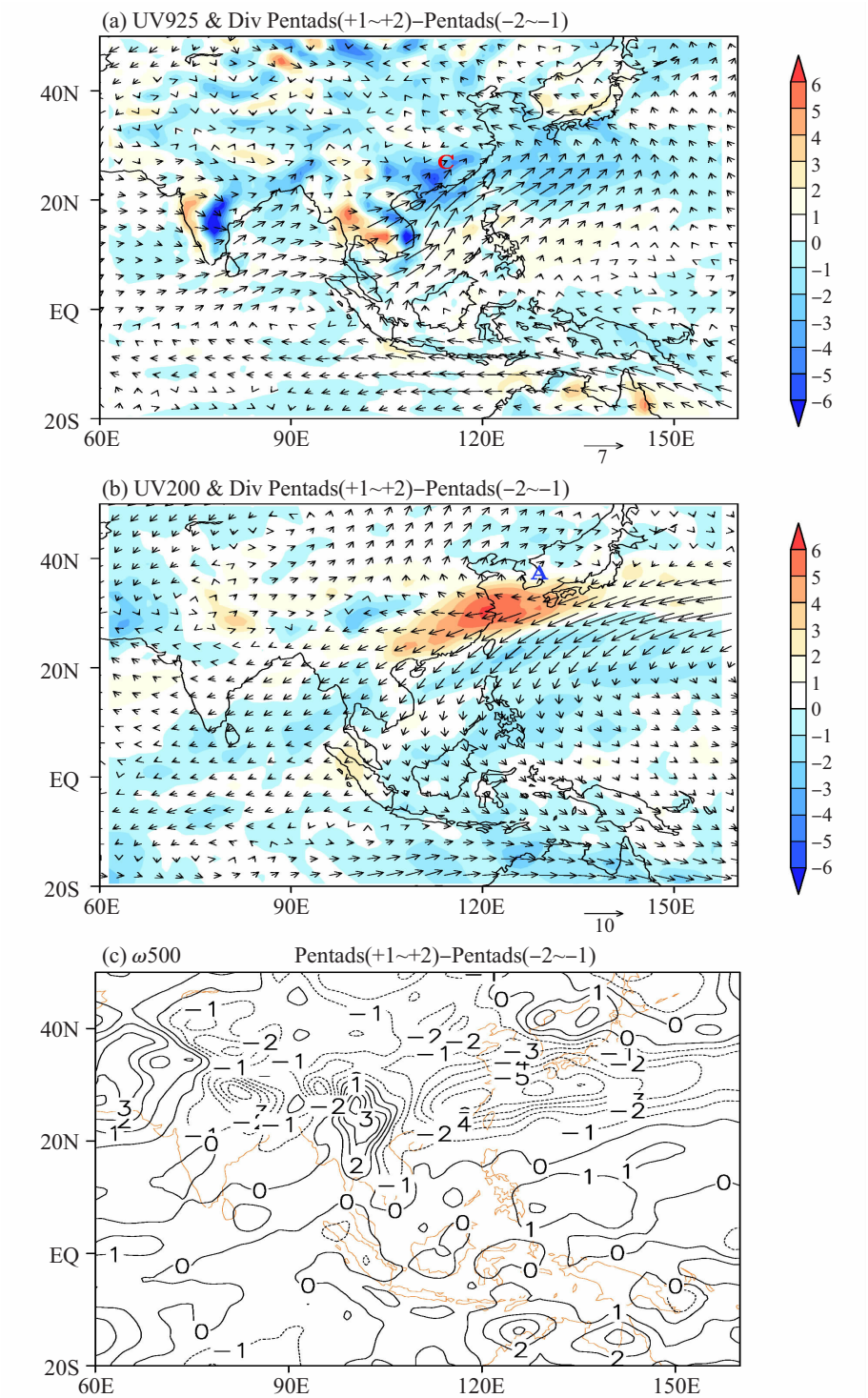

Figure 5. Differences of wind and p-velocity before and after the WST. (a) and (b) are the 925-hPa and 200-hPa horizontal wind (m s^{-1}) as well as their divergence (shading; 10^{-6} s^{-1}), respectively. "C" and "A" denote the centers of cyclone and anticyclone, respectively. (c) 500-hPa p-velocity (10^{-6} Pa s^{-1}).

3.2.2 RELATIONSHIP BETWEEN WST AND PRECIPITATION

The correlation coefficients between WSTT and spring precipitation, and monthly precipitation from March to June are calculated for further understanding of the connection between the WSTT and the precipitation over the SC-NSCS. There is a significant negative correlation in southeastern China, while a significant positive correlation in southwestern China (Fig. 6a). These results suggest that the earlier transition, associated with the earlier onset of rainy season, brings more spring rainfall over southeastern China, and a reverse situation occurs in southwestern China. In addition, the correlation in southern China is only significant in March (Fig. 5b) among the three months from March to May. The reason might be that the climatological WSTT is in mid-March (Pentad 14), therefore the year-to-year variation of WSTT exerts mainly influence in the rainfall in March. In contrast, the WSTT has a weak relationship with the rainfall in April and May. However, the WSTT has a significant negative correlation with precipitation over southern China in June (Fig. 5c).

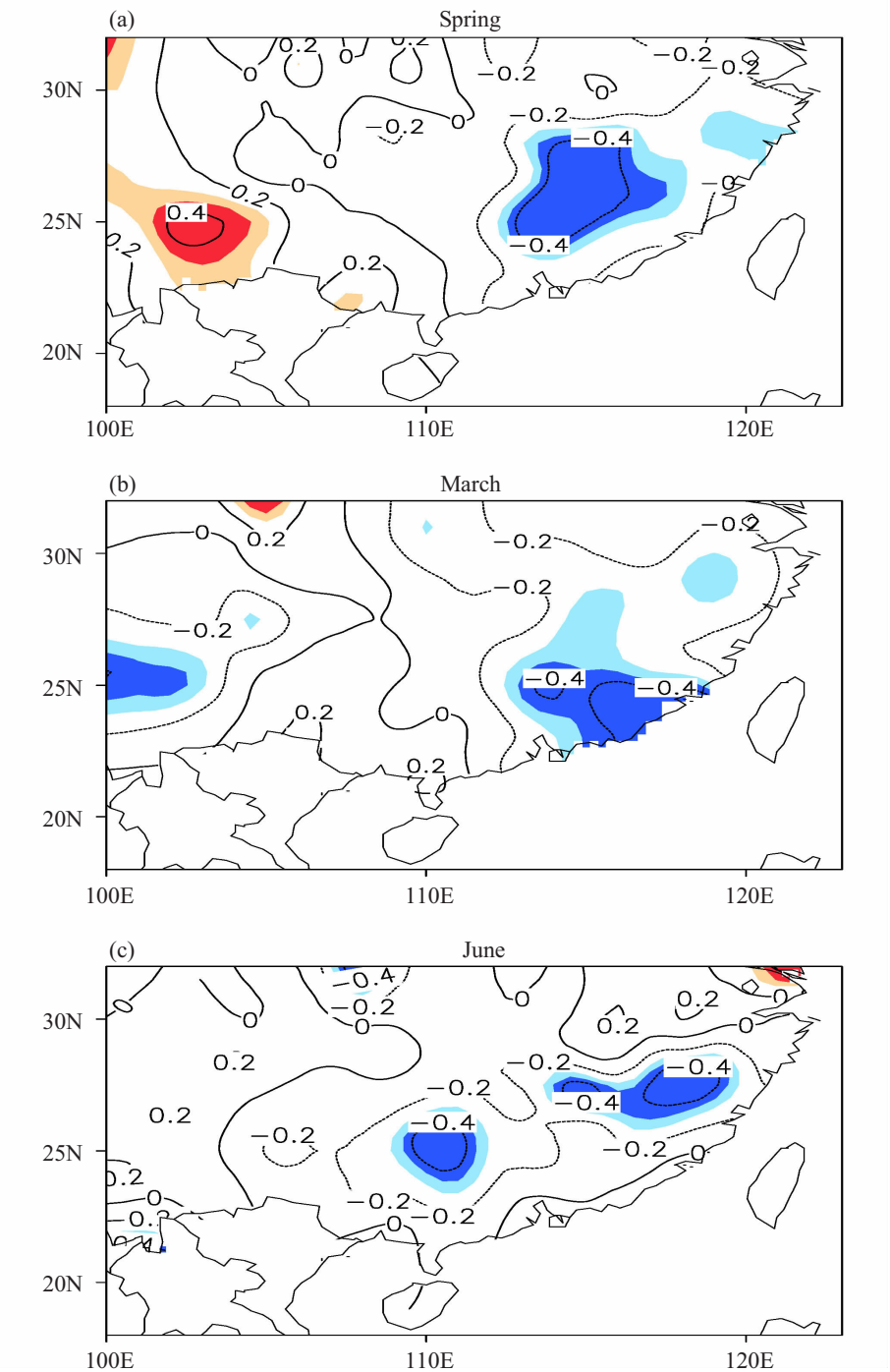

Figure 6. Correlation coefficients between WSTT and the precipitation in (a) spring (March to May), (b) March and (c) June, respectively. Orange and light blue shadings show the areas with 90% confidence level, while red and dark blue shadings show the areas with 95% confidence level of student *t*-test.

However, the relationship between the WSTT and the precipitation on pentad time scale seems to be much more complicated (Fig. 7). The negative correlation between the WSTT and the regionally averaged precipitation over southeastern China (113°–120°E, 22°–27° N) is only significant in the first three pentad of March. The relationship turns much more complicated in April and May, only the fifth pentad of April and the third pentad of May are significant.

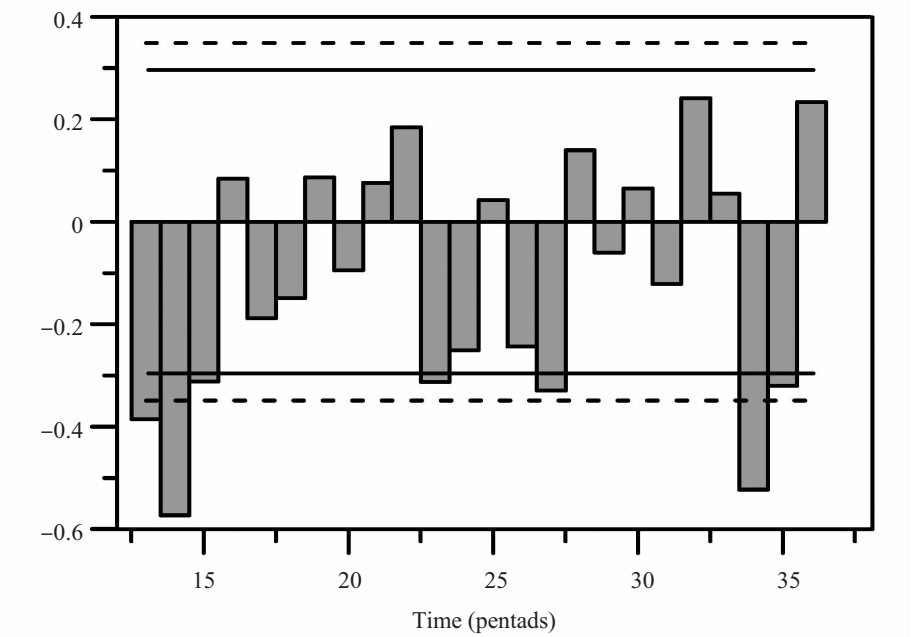

Figure 7. Correlation coefficients between WSTT and the pentad precipitation averaged (113°–120°E, 22°–27°N) during Pentads 13 to 36. The dashed and solid lines show the 95% and 90% confidence level, respectively.

3.2.3 CHARACTERISTICS OF ATMOSPHERIC CIRCULATION RELATED TO INTERANNUAL VARIATION OF WST

Based on a criterion of 1.0 times of the standard deviation of the WSTT, six early WST years (1983, 1992, 1994, 1998, 2009 and 2010) and five late WST years (1985, 1997, 1999, 2003 and 2008) are figured out from the normalized WSTT at 925 hPa in Fig. 4.

Figure 8 shows the composite anomalies of wind, divergence and vertical motion in March for the early WST years. At the low level, an anomalous cyclone is observed over southeastern China, while anticyclonic wind anomalies are over the SCS (Fig. 8a). This circulation pattern is conducive to transporting more moisture to the coastal areas of southeastern China and inducing more precipitation over there. Meanwhile, southern China are also under the influence of a striking anomalous cyclone at the high level (Fig. 8b), with an abnormal divergence zone over southeastern China and the East China Sea, which is favorable for the abnormal low-level convergence and ascending motion (Fig. 8c). In contrast, abnormal sinking motion prevails over the eastern part of Maritime Continent. The anomalous circulation patterns of late WST years are roughly the opposite of early years (not shown).

Figure 9 shows the composite anomalies of velocity potential at 925 hPa and 200 hPa in March of early WST years. Again, we can see there are convergence anomalies over southern China, and divergence anomalies over the western tropical Pacific Ocean at 925 hPa (Fig. 9a). The divergent winds flow from the western tropical Pacific to southern China. In addition, it is important to note that on a larger scale, over the central eastern tropical Pacific Ocean it is an anomalous convergence center. This distribution pattern of velocity potential anomalies is like that associated with ENSO. At 200 hPa, it is common to observe opposite anomalies of divergence and convergence and divergent winds in the above-mentioned regions. The patterns of velocity potential anomalies for the later WST years are approximately the opposite of early years (not shown). Besides, four of the six early WST years (excluding 1994 and 2009) and three of the five late WST years (excluding 1997 and 2003) are El Niño and La Niña decaying years, respectively. Thus, it appears that ENSO is a main cause of anomalous circulation and convection over the western Pacific and anomalous rainfall over the SC-NSCS in anomalous WST years.

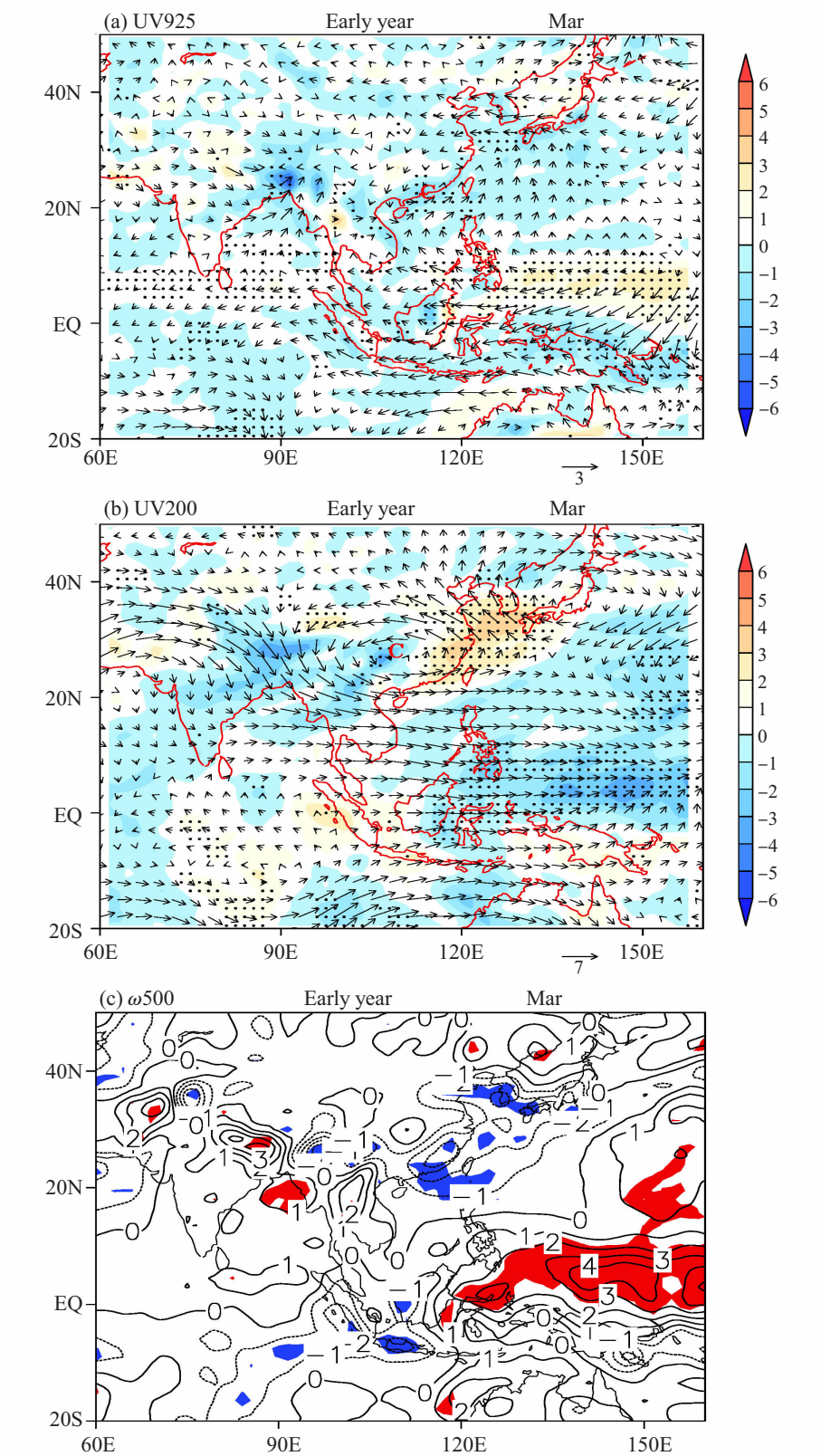

Figure 8. (a) 925-hPa wind anomalies (m s^{-1}) and their divergence (shading; 10^{-6} s^{-1}) in March of early WST years; (b) the same as (a) but for 200 hPa; (c) the same as (a) but for *p*-velocity at 500 hPa (10^{-6} Pa s^{-1}). Stippling in (a) and (b) and shading in (c) indicate the 95% confidence level.

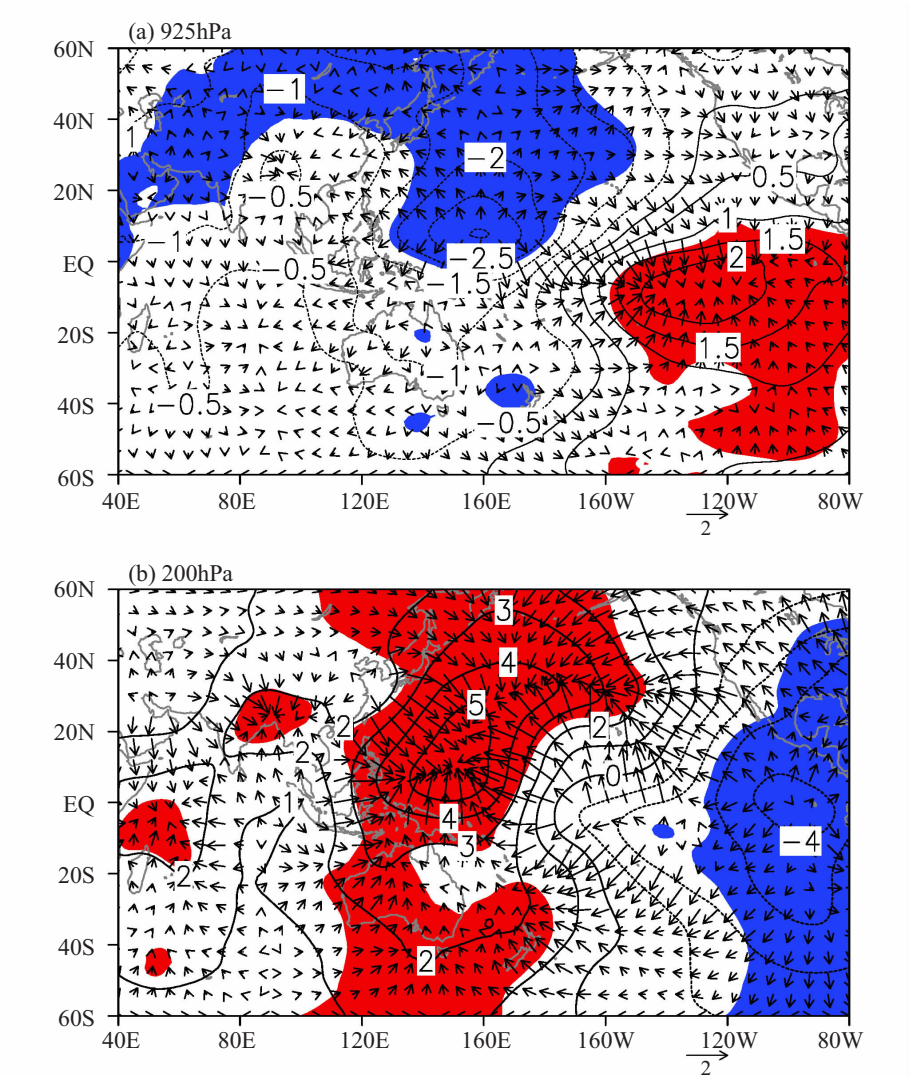

Figure 9. Composite anomalies of velocity potential (contours, 10^6 m^2 s^{-1}) and divergence wind (vectors, m s^{-1}) at (a) 925 hPa and (b) 200 hPa in March of early WST years. Shading indicates the velocity potential anomalies at 95% confidence level.

4 INFLUENCE OF TROPICAL PACIFIC SST ANOMALIES ON WST

To understand the interannual relationship between WST and ENSO, Fig. 12 shows the lagged regression of SST anomalies against the normalized WSTT series from previous December to following May separately. There are some notable common features in SST anomalies evolving from December to May. First, prominent negative SST anomalies are observed in the central-eastern equatorial Pacific with decaying amplitudes from December to May, while there are significant positive SST anomalies in the western tropical Pacific. Second, there are notably intensified negative SST anomalies in the tropical Indian Ocean from February to May. The afore-mentioned seasonal evolution of SST anomaly patterns is actually associated with the decaying phase of ENSO events, which may be further confirmed by high correlation coefficients of −0.91 and −0.86 between WSTT and the SST anomaly in the Niño3.4 region (170°−120°W, 5°S−5°N) in winter and spring, respectively, and this results suggest that cold/warm ENSO events may induce late/early WSTs over the SC-NSCS. The impact process of ENSO on the WST can be simply illustrated as follows: according to the results of Wang et al. [23], during the decaying phase of warm ENSO events, the positive SST anomalies in central-eastern equatorial Pacific may induce an anomalous anticyclone over the Philippines Sea and nearby area via a Rossby wave-type response, just as shown in Fig. 8a. The anomalous anticyclone is conducive to the moisture transport from the tropics to southern China, and at the same time, the southwest wind anomalies from the northern SCS and the north wind anomalies from the north meet over southern China to induce more rainfall in spring, especially in March, finally. Besides, the anomalous southwest wind is favorable to spring onset in southern China, i.e., the WST.

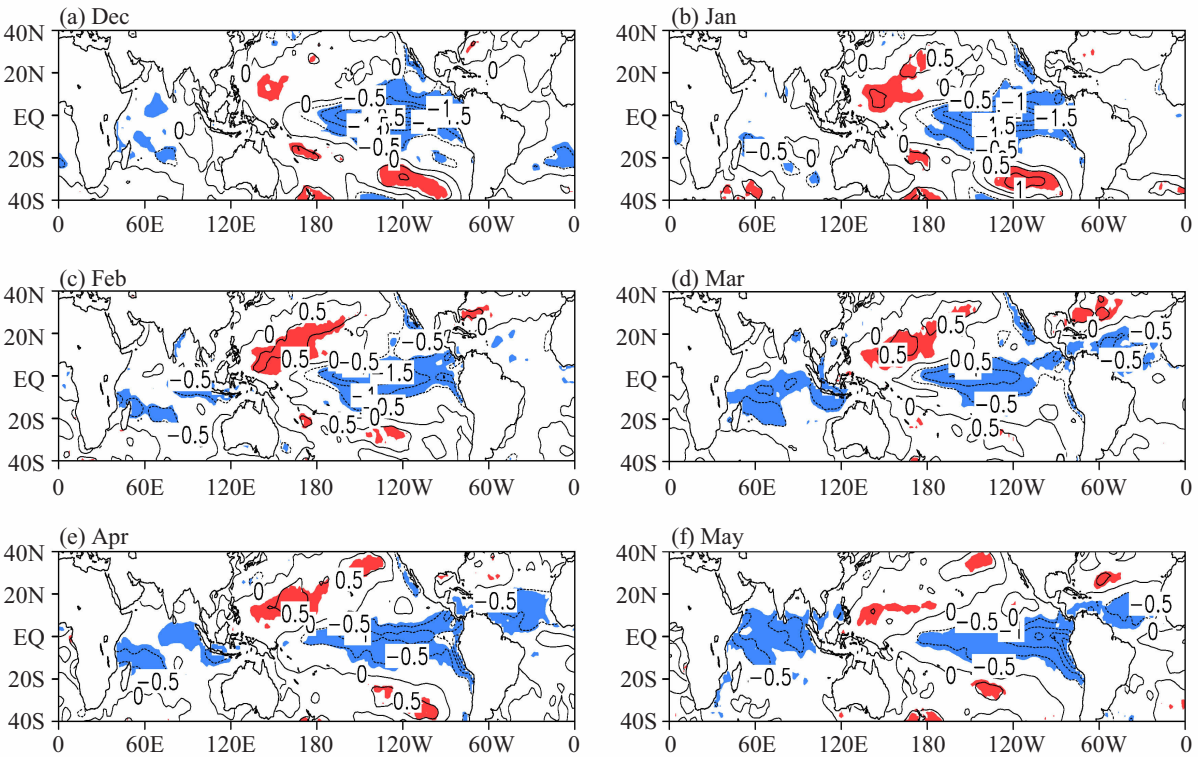

Figure 10. Linear regression coefficients (0.1*K*) of monthly mean SST anomalies against the normalized time series of WSTT. (a)-(f) are for previous December to following May, respectively. Shading indicates the areas at 95% confidence level of *F*-test.

5 SUMMARY

In this study, we investigated the climatological features of the WST over southern China and its surrounding areas as well as its interannual variation. The relationship between the seasonal transition and the precipitation over southern China, and the possible mechanism for the interannual variability were also discussed.

The climatological mean WSTT is approximately in mid-March (Pentad 14) over southern China and the northern SCS, and at the end of March (Pentad 18) over northern China, while it is quite complicated over central China.

During the seasonal transition stage, anomalous southwest winds prevail at low-level over southern China and its nearby regions with enhanced convergence center over southern China, bringing more moisture from the BOB and SCS to southern China; meanwhile, the upper level is under the influence of an obvious divergence wind pattern over southern China to the southwest part of Japan presents, and enhancing upward motion. All the change of circulation is favorable for more precipitation over southern China after the seasonal transition.

The WST locates predominantly on the interannual variation over southern China and the northern SCS. Early WST, i.e., early spring onset, may induce more precipitation over southern China in spring, especially in March, while late WST will result in less precipitation. The interannual variability of WST and the related large-scale circulation are closely associated with the decaying phase of ENSO events. The El Niño events contribute to anomalous Philippines anticyclone, which is conducive to an early WST and more precipitation over southern China.

There are still some issues remained to be discussed. The relationship between the WST and the precipitation of the late spring or early summer is worth further discussing. As shown in Fig. 6, the negative correlation between WSTT and the precipitation in June over southern China is also prominent. The mechanism of this phenomenon is ignored in the present study and should be fully investigated in future. The relations of the second leading EOF mode of WSTT with the circulation and precipitation over East Asian monsoon region, and the mechanism also need further study.

Acknowledgments: The authors thank the two anonymous reviewers for their constructive comments that greatly helped the improvement of the paper. This work was jointly supported by the National Key Basic Research Program of China (2014CB953901), Program of National Science Foundation of China (41475049) and Fundamental Research Funds for the Central Universities (16lgjc05). This work was also supported by the Jiangsu Collaborative Innovation Center for Climate Change.

REFERENCES:

[1] CHEN L X, JIN Z. The medium-range variation of the summer monsoon circulation system over East Asia [J]. Adv Atmos Sci, 1984, 1(2): 224-233.

[2] ZHU Q G, HE J, WANG P. A study of circulation

differen ce between East Asian and Indian summer monsoon with their interaction [J]. Adv Atmos Sci, 1986, 3(4): 465-477.
[3] TAO S Y, CHEN L X. A review of recent research on the East Asian summer monsoon in China [M]// CHANG C P, KRISHNAMURTI T N (eds), Monsoon Meteorology. London: Oxford University Press, 1987, 60-92.
[4] LAU K M, YANG S. Climatology and interannual variability of the southeast Asian summer monsoon [J]. Adv Atmos Sci, 1997, 14(2): 141-162.
[5] WEBSTER P J, MAGANA V O, PALMER T N, et al. Monsoon: processes, predictability and the prospects for prediction [J]. J Geophys Res, 1998, 103 (C7): 14451-14510.
[6] WANG B, LIN H. Rainy season of the Asian-Pacific summer monsoon [J]. J Climate, 2002, 15(4): 386-398.
[7] WU G X, WANG J, LIU X, et al. Numerical modeling of the influence of Eurasian orography on the atmospheric circulation in different seasons [J]. Acta Meteor Sinica, 2005, 63(5): 603-612 (in Chinese).
[8] TIAN S F, YASUNARI T. Climatological aspects and mechanism of spring persistent rains over central China [J]. J Meteor Soc Japan, 1998, 76(1): 57-71.
[9] WAN R J, WU G X. On the mechanism of spring persistent rains [J]. Sci in China (Ser D), 2006, 36(10): 936-950.
[10] ZHAO P, ZHANG R, LIU J, et al. Onset of southwesterly wind over eastern China and associated atmospheric circulation and rainfall [J]. Climate Dyn, 2007, 28(7-8): 797-811.
[11] JIAN M Q, LUO H, QIAO Y. Seasonal variability of atmospheric heat sources over the Asian-Australian Monsoon region [J]. Acta Scientiarum Naturalium Universitatis Sunyatseni, 2004, 43 (3): 106-109 (in Chinese).
[12] QI L, HE J, ZHANG Z, et al. Seasonal cycle of the zonal land-sea thermal contrast and East Asian subtropical monsoon circulation [J]. Chin Sci Bull, 2008, 53 (1): 131-136.
[13] ZHU Z W, HE J, QI L. Seasonal transition of East Asian subtropical monsoon and its possible mechanism [J]. J Trop Meteor, 2012, 18(3): 305-313.
[14] YAN Z W, XIA J, QIAN C, et al. Changes in seasonal cycle and extremes in China during the period 1960 – 2008 [J]. Adv Atmos Sci, 2011, 28(2): 269-283.
[15] ZHENG H F, NEIL B M, HE X, et al. Temporal and geographical variation in the onset of climatological spring in northeast China [J]. Theor Appl Climatol, 2013, 114(3-4): 605-613.
[16] HO C H, LEE E, LEE I, et al. Earlier spring in Seoul, Korea [J]. Int J Climatol, 2006, 26(14): 2117-2127.
[17] ZHENG J Y, GE Q, HAO Z, et al. Spring phenophases in recent decades over eastern China and its possible link to climate changes [J]. Climatic Change, 2006, 77 (3-4): 449-462.
[18] WU T W, QIAN Z. The relation between the Tibetan winter snow and the Asian summer monsoon and rainfall: An observational investigation [J]. J Climate, 2003, 16(12): 125- 134.
[19] CHEN W, WANG L, XUE Y, et al. Variabilities of the spring river runoff system in eastern China and their relations to precipitation and sea surface temperature [J]. Int J Climatology, 2009, 29(10): 1381-1394.
[20] ZHOU L T. Impact of East Asian winter monsoon on rainfall over southeastern China and its dynamical process [J]. Int J Climatol, 2011, 31(5): 677-686.
[21] ZHANG R, SUMI A, KIMOTO M. Impact of El Niño on the East Asian monsoon: A diagnostic study of the '86/87 and '91/92 events [J]. J Meteor Soc Japan, 1996, 74(1): 49-62.
[22] ZHANG R, SUMI A, KIMOTO M. A diagnostic study of the impact of El Niño on the precipitation in China [J]. Adv Atmos Sci, 1999, 16(2): 229-241.
[23] WANG B, WU R, FU X. Pacific-East Asia teleconnection: How does ENSO affect East Asian climate? [J]. J Climate, 2000, 13(9): 1517-1536.
[24] WU R G, HU Z, KIRTMAN B P. Evolution of ENSO-related rainfall anomalies in East Asia [J]. J Climate, 2003, 16(22): 3742-3758.
[25] ZHOU L T, WU R. Respective impacts of East Asia winter monsoon and ENSO on winter rainfall in China[J]. J Geophys Res, 2010, 115, doi: 10.1029/2009JD012502.
[26] SUN C, YANG S. Persistent severe drought in southern China during winter-spring 2011: Large-scale circulation patterns and possible impacting factors [J]. J Geophys Res, 2012, 117, doi: 10.1029/2012JD017500.
[27] YANG Q. Impact of the Indian Ocean subtropical dipole on the precipitation of east China during winter monsoons[J]. J Geophys Res, 2009, 114, doi: 10.1029/2008JD011173.
[28] ZHOU L T, TAM C, ZHOU W, et al. Influence of South China Sea SST and the ENSO on winter rainfall over South China [J]. Adv Atmos Sci, 2010, 27(4): 832-844.
[29] CHEN L T, WU R. Interannual and decadal variations of snow cover over Qinghai-Xizang Plateau and their relationships to summer monsoon rainfall in China [J]. Adv Atmos Sci, 2000, 17(1): 18-30.
[30] GONG D Y, WANG S, ZHU J. East Asian winter monsoon and Arctic Oscillation [J]. Geophys Res Lett, 2001, 28(10): 2073-2076.
[31] WU R G, YANG S, WEN Z, et al. Interdecadal change in the relationship of southern China summer rainfall with tropical Indo-Pacific SST [J]. Theor Appl Climatol, 2012, 108(1-2): 119-133.
[32] SMITH T M, REYNOLDS R W, PETERSON T C, et al. Improvements to NOAA's historical merged land-ocean surface temperature analysis (1880-2006) [J]. J Climate, 2008, 21(10): 2283-2296.
[33] DEE D P, UPPALA S M, SIMMONS, A J, et al. The ERA-Interim reanalysis: Configuration and performance of the data assimilation system [J]. Quart J Roy Meteor Soc, 2011, 137(656): 553-597.
[34] ZENG Q C, ZHANG B. On the seasons of general atmospheric circulation and their abrupt changes, Part I: General concept and method [J]. Scientia Atmospherica Sinica, 1992, 16(6): 641-648 (in Chinese).
[35] NORTH G R, BELL T L, CAHALAN R F, et al. Sampling errors in the estimation of empirical orthogonal functions [J]. Mon Wea Rev, 1982, 110(7): 699-706.

Citation: ZHOU Ming-sen and JIAN Mao-qiu. Interannual variability of winter-to-spring circulation transition over southern China and its surrounding areas and mechanisms [J]. J Trop Meteor, 2019, 25(4): 471-482.